TU Delft

Reactor Institute Delft

Faculty of Applied Physics

Investigating the Selective Separation Ability of an Optimized Microfluidic Chip with Focus on Metal Ions

Author:
Paul F.W. Möller

Committee Members:
Prof.dr.ir. Jan Leen Kloosterman
Dr.ir. Martin Rohde
Zheng Liu (Supervisor)

September 3, 2017

TU Delft

Nomenclature

Alphabetic Physics Constants

c	Concentration	mol/m^3
d	Extraction channel height	μm
$\mathbb{D}$	Diffusion coefficient	m^2/s
ER	Extraction rate	%
f	frictional force	N
h	Extraction channel full-width	μ
k	Mass transfer coefficient	m/s
k_b	Boltzmann constant	J/K
L	Extraction channel length	mm
L_{pen}	Penetration depth	μm
m	Partition coefficient	–
M	Total mass	kg
p	Pressure	Pa
Q	Volumetric flow rate	m^3/s
r	Radius	μm
t	Time	s
T	Temperature	T
v	Velocity	m/s
w	Extraction channel half-width	m^3/s

Greek Alphabetic Physics Constants

γ	Interfacial tension	N/m
Δ	Difference	–
η	Viscosity	$mPa \cdot s$
θ	Contact angle	$^\circ$
ρ	Density	kg/m^3
ϕ	Flow rate	s^{-1}
ϕ''	Diffusive flux	$mol/(m^2 s)$
Ω	Fixed shaped region	–

Vectors, tensors and others

D_t	Material time derivative
$\mathbf{E}$	Electric field
$\mathbf{f}$	Force density
M	Metal specie
$[M]$	Concentration of specie
R	Rest group
$\overline{R}$	Rest group in organic phase
$\mathbf{v}$	Velocity field
σ'	Viscous stress tensor

Subscripts

abs	Absolute value
aq	Aqueous phase
el	Electric
ex	Extraction
$grav$	Gravitation
i	interface
in	Inlet
in	Outlet
org	Organic phase
$press$	Pressure
rel	Relative value
vis	viscosity
x	x-direction

Abstract

In the Reactor Institute of Delft, the process of gaining Molybdenum-99 from the irradiation of low enriched Uranium-235 solution for medical purposes is being investigated. When Molybdenum-99 decays the isotope Technetium-99m can be obtained. This isotope is widely used for medical imaging. Due to the half-life time of 6 hours it is not suitable for transport and that is where Molybdenum-99 comes in. This isotope has a half-life time of 66 hours and is therefore much more suitable for transportation.

When the low enriched Uranium-235 solution is irradiated a large amount of fission products will arise. Molybdenum-99 should therefore be solely separated from these other fission products. One method of extracting species from an aqueous solution is liquid-liquid extraction on micro scale. This method is bases on the immiscibility of two phases, normally an aqueous phase in which the to be separated specie is dissolved and an organic phase. The small dimensions of the system allow for example for a large interfacial area to volume ratio, short diffusion distance and rapid stabilization of the interface.

In previous published work by S. Goyal et al liquid-liquid extraction is used with an extractant present in the organic phase. This extractant is known as HOBO and selectively bounds to copper(II) ions. The work claims an extraction rate of exceeding 95 % for a channel length of 7 millimeters and an average residing time of 0.21 seconds.

This research will focus on this variant of liquid-liquid extraction, which is referred to as active liquid-liquid extraction. Investigation is done on the parameters of the channel to find the optimized parameter combination and predict the extraction rate. Next to this also the qualitative influence of the parameters is investigated. It is done by the hand of a model made in COMSOL® which is evaluated by comparing it to known studies and test it with analytical approaches.

After validating the model a parametric sweep is made. The length, width and height of the channel as well as the viscosity of the organic phase, the diffusion coefficient in the aqueous phase and the aqueous flow rate are swept for several values. These values are restricted to account for the known limitations on their values. The large data obtained is analyzed to find the optimal setup and to deduce the qualitative influence of the parameters.

It is found that a small width and a large height and length are optimal for the dimensions of the extraction channel. Furthermore, a low flow rate, a high diffusion coefficient and a large organic viscosity value relative to the aqueous viscosity show an optimum for the phase parameters. Keeping the limitations on the values in mind the optimal setup will result in an extraction rate of 72 percent. Additionally, it has been deduced that changing the organic viscosity has the least amount of influence on the extraction rate, while changing the width caused the most influence. If the limitations on the length and the width are taken out of consideration an extraction rate of 99 percent for an extraction channel length of 4 cm is found. For the width, an extraction percentage of 90 will be found when the width is narrowed down to 20 μm. Furthermore, it has been demonstrated that the mentioned extraction rate in the work of S. Goyal et al cannot be achieved in the way it has been interpreted in this research. This research found an extraction rate of less than 10 percent which has been justified by an analytical approximation.

Contents

Introduction

One of the projects currently running in the Reactor Institute of Delft (RID) is the process of gaining Molybdenum-99 from the irradiation of low enriched Uranium-235 solution for medical purposes. Molybdenum-99 is an isotope that is formed by the decay of a fission product of Uranium-235 and has a half-life of 66 hours. It is the parent isotope of Technetium-99m, which is widely used for medical imaging [16]. Because this isotope has a half-life of 6 hours it is not suitable as a transport product. This were Molybdenum-99 and especially its longer half-life comes in. Molybdenum-99 is transported and when Technetium-99m is required it can be retrained from a so-called Mo-Tc generator.

In order to obtain Molybdenum-99 it should be separated from the other fission products. A well-known method to achieve this is called liquid-liquid extraction. This is an extraction method based on the immiscibility of two liquid phases. Especially liquid-liquid extraction on micro scale has proved its usefulness [6]. The small dimensions of the system allow for a large interfacial area to volume ratio, short diffusion distance and rapid stabilization of the interface. Next to all this only small volumes of both phases are needed in compare with liquid-liquid extraction done in large containers. This means a small amount of radio-active substances can be used, which is an advantage.

In study done by A. Blok [4] the separation of Technetium-99m in a microfluidic chip was examined. A numerical model, bounded to several restrictions, was made in MATLAB® and eventually the model was tested in practice. The practice showed that a bad phase separation was found for flow rates lower than 10 $\mu L/min$.

Study done by S. Goyal et al [8] examined the separation of copper in a microfluidic chip with the help of an active variant of liquid-liquid extraction. The extractant used in this study is known as 2-hydroxy-4-n-octyloxybenzophenone oxime and better know as HOBO. The experiment was done in practice and evaluated with a model made in COMSOL®. For an extraction channel of 7 millimeters the extraction rate often exceeded 95 percent, while a study done by G. Hellé [9] found that for an extraction channel of 8 centimeters the extraction rate was around 76 percent. In this case U(VI) was separated with the extractant Aliquat® 336.

In this research, active microfluidic liquid-liquid extraction, which is assumed to be more efficient than the non-active variant, to extracted especially metal ions will be investigated more with the help of a model made in COMSOL® to optimize its use in the separation process of metals. The focus is on finding the qualitative influences of the tunable parameters of the microfluidic chip and the phases involved. The modeled Y-shaped microfluidic chip will receive an aqueous solution with a solute (metal ions) on one inlet and an organic solution without solute on the other inlet. At the outlets, the amount of separated metal ions will be calculated from which the extraction rate will be deduced. The model will be tested to other known studies and will be verified with known microfluidic physics to ascertain the correctness. To gain insights in the mechanism of the microfluidic solvent extraction topics like mass transfer, fluid flow and interfacial reactions will be discussed.

1 | Theory

1.1 Microfluidics

Microfluidics is the field of physics that deals with fluid motion in lab-on-a-chip systems. This section will discuss all the relevant fluid physics in this field of work. First the general physics will be discussed and from there on the focus will be on the laminar two-phase flow situation.

1.1.1 The continuity equation for (in)compressible fluids

Consider a randomly fixed shaped region Ω within a liquid as H. Bruus [5] indicates. The total mass of the liquid in this region can be found by the volume integral over the density ρ,

$$M(\Omega, t) = \int_{\Omega} d\mathbf{r}\rho(\mathbf{r}, t), \tag{1.1.1}$$

where $d\mathbf{r}$ is the infinitesimal integration volume. Change in mass can only occur by mass flow from or to the region. This can be described by the mass current density $\mathbf{J}$,

$$\mathbf{J}(\mathbf{r}, t) = \rho(\mathbf{r}, t)\mathbf{v}(\mathbf{r}, t), \tag{1.1.2}$$

wherein $\mathbf{v}$ denotes the Eulerian velocity field. The time-derivative of the total mass can be calculated by taking the time-derivative of equation 1.1.1

$$\frac{\partial M(\Omega, t)}{\partial t} = \int_{\Omega} d\mathbf{r}\frac{\partial \rho(\mathbf{r}, t)}{\partial t}. \tag{1.1.3}$$

It can also be calculated by taking the surface integral over $\partial\omega$ of J. This will lead to, with the help of Gauss theorem,

$$\frac{\partial M(\Omega, t)}{\partial t} = -\int_{\Omega} d\mathbf{r}\nabla \cdot (\rho(\mathbf{r}, t)\mathbf{v}(\mathbf{r}, t)). \tag{1.1.4}$$

The minus sign is obtained due to the fact that the mass inside the region will decrease when $\rho\mathbf{v}$ is parallel to the outward pointing surface vector $\mathbf{n}$. Subtracting equation 1.1.4 from equation 1.1.3 will lead to,

$$\int_{\Omega} d\mathbf{r}\left[\frac{\partial \rho(\mathbf{r}, t)}{\partial t} + \nabla \cdot (\rho(\mathbf{r}, t)\mathbf{v}(\mathbf{r}, t))\right] = 0. \tag{1.1.5}$$

This can only be zero if the term between brackets equals zero and this will finally lead to the know continuity equation,

$$\frac{\partial \rho(\mathbf{r}, t)}{\partial t} + \nabla \cdot (\rho(\mathbf{r}, t)\mathbf{v}(\mathbf{r}, t)) = \frac{\partial \rho(\mathbf{r}, t)}{\partial t} + \nabla \cdot \mathbf{J} = 0 \tag{1.1.6}$$

Because microfluidic devices cannot withstand high velocities due to the forces coming along the velocity is much slower than the velocity of sound in the fluid. Because of this we can treat the fluids as incompressible, which results in the fact that ρ is constant and equation 1.1.6 simplifies to,

$$\nabla \cdot \mathbf{v} = 0. \tag{1.1.7}$$

This will be referred to as the incompressible continuity equation.

1.1.2 The Navier-Stokes equation

The Navier-Stokes equation is Newton's second law for fluid particles. Newton's 'normal' second law is known as

$$m\frac{d\mathbf{v}}{dt} = \sum_j \mathbf{F_j}. \tag{1.1.8}$$

In fluid mechanics, and thus in microfluidics, this will be divided by the volume of the fluid and therefore it will be expressed in ρ and the force densities $\mathbf{f_j}$. The time-derivative of the velocity field $\mathbf{v}$ will also differ, due to the fact that $\mathbf{v}$ is not the velocity of an individual fluid particle. The correct equations for the force densities $\mathbf{f_j}$ and the time-derivative of $\mathbf{v}$, better known as the material time-derivative D_t, will therefore firstly be derived.

The total differential of the Eulerian velocity field yields

$$d\mathbf{v} = dt\frac{\partial \mathbf{v}}{\partial t} + (d\mathbf{r}\cdot\nabla)\mathbf{v}. \tag{1.1.9}$$

$d\mathbf{r}$ should be denoted as $d\mathbf{r} = \mathbf{v}dt$ since the flow of an individual fluid particle should be calculated. This substitution finally reveals the expression for the material time-derivative,

$$D_t = \frac{\partial}{\partial t} + (\mathbf{v}\cdot\nabla). \tag{1.1.10}$$

The forces acting upon the region Ω can be divided in four force categories, namely the gravitational force density ($\mathbf{f}_{grav}$), the electrical force density ($\mathbf{f}_{el}$), the pressure force density ($\mathbf{f}_{press}$) and the viscosity force density ($\mathbf{f}_{vis}$). The first two are obtained real easy, namely the density ρ times the gravitational force $\mathbf{g}$ and the electrical density ρ_{el} times the electric field $\mathbf{E}$ for respectively $\mathbf{f}_{grav}$ and $\mathbf{f}_{el}$. So, added together leaves us with,

$$\sum_j \mathbf{f_j} = \mathbf{f}_{grav} + \mathbf{f}_{el} + \mathbf{f}_{press} + \mathbf{f}_{vis} = \rho\mathbf{g} + \rho_{el}\mathbf{E} + \mathbf{f}_{press} + \mathbf{f}_{vis}. \tag{1.1.11}$$

The total external pressure force working on the region Ω due to the pressure p is given by the surface integral of $\mathbf{n}p$,

$$\mathbf{F}_{press} = \int_{\partial\Omega} da\mathbf{n}(-p) = \int d\mathbf{r}(-\nabla p). \tag{1.1.12}$$

The minus sign can be explained due to the fact that $\mathbf{n}p$ is the force per area from the region acting on the surroundings. The minus sign is thus added to depict the opposite. The integrand of the above integral is actually the pressure force density and thus,

$$\mathbf{f}_{press} = -\nabla p. \tag{1.1.13}$$

In the much of the same way the viscous force $\mathbf{F}_{vis}$ can be written as the surface integral, which converts to a volume integral with the help of Gauss like

$$\mathbf{F}_{vis} = \int_{\partial\Omega} da n_k \sigma'_{ik} = \int_\Omega d\mathbf{r}\frac{\partial \sigma'_{ik}}{\partial k}, \tag{1.1.14}$$

in which n_k is the normal vector in the k-direction and σ'_{ik} is the ik^{th} element of the viscous stress tensor. This viscous stress tensor looks like $\sigma'_{ik} = \eta\left(\frac{\partial v_i}{\partial k} + \frac{\partial v_k}{\partial i} - \frac{2}{3}\delta_{ik}\frac{\partial v_j}{\partial j}\right)$. With the fact that the liquid is incompressible the viscous force density will eventually come down to

$$\mathbf{f}_{vis} = \eta\nabla^2\mathbf{v} \tag{1.1.15}$$

All density forces are now known and together with the knowledge about the material time-derivative the incompressible Navier-Stokes equation results in [5],

$$\rho\left(\frac{\partial \mathbf{v}}{\partial t} + (\mathbf{v}\cdot\nabla)\mathbf{v}\right) = \sum_j \mathbf{f}_j. \tag{1.1.16}$$

1.1.3 Two-Phase Poiseuille flow

The flow through the microfluidic chip in this case will be a parallel side-by-side two-phase flow. As stated earlier, two separate inlets will be used. Because of the immiscibility of these fluids an interface will arise somewhere in the middle of the microfluidic chip. In this case the interface will be assumed to be exactly in the middle of the chip. This will be modeled by using an one-phase flow of which the viscosity and density are space-dependent. To know if the model returns physical valuable results understanding about two-phase flow is needed.

Let us now focus on the velocity profile in the center of the chip, the part were both fluids meet. Figure 1.1.1 shows this area of the microfluidic chip. Note that in this case h^* equals $\frac{1}{2}h$, due to the fact that the interface lies in the middle. For obtaining the velocity profile shown in figure 1.1.1 several boundary conditions should be defined first,

$$\text{No slip at the walls} : v_{1,x}(0) = v_{2,x}(h) = 0, \tag{1.1.17a}$$

$$\text{Continuous velocity at the interface} : v_{1,x}\left(\frac{1}{2}h\right) = v_{2,x}\left(\frac{1}{2}h\right), \tag{1.1.17b}$$

$$\text{Continuous shear stress at the interface} : \eta_1 \frac{\partial v_{1,x}}{\partial z}\left(\frac{1}{2}h\right) = \eta_2 \frac{\partial v_{2,x}}{\partial z}\left(\frac{1}{2}h\right). \tag{1.1.17c}$$

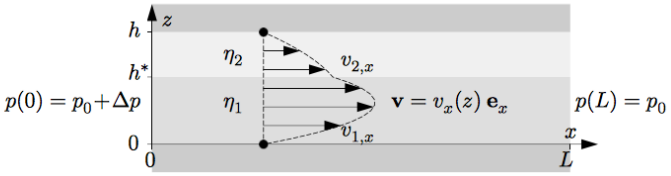

Figure 1.1.1: The middle part of a microfluidic chip. h denotes the width of the microchannel, whereas x denotes the length of the channel. η_1 and η_2 represent respectively the viscosity of the organic fluid and the aqueous fluid. $v_{1,x}$ and $v_{2,x}$ represent the velocity in the x-direction. [5]

Herein are $v_{1,x}$ and $v_{2,x}$ the velocities for respectively the organic and the aqueous fluid. η_1 and η_2 are the corresponding viscosities and h denotes the width of the channel. Using for both velocities the known infinite parallel-plate channel velocity formula [5],

$$v_x(z) = \frac{\Delta p}{2\eta L}(h - z)z, \tag{1.1.18}$$

the equations, using the boundary conditions 1.1.17a and 1.1.17b and for the two velocities will become,

$$v_{1,x}(z) = \frac{\Delta p}{2\eta L}(h_1 - z)z, \tag{1.1.19a}$$

$$v_{2,x}(z) = \frac{\Delta p}{2\eta L}(h - z)(z - h_2). \tag{1.1.19b}$$

Using boundary condition 1.1.17c will solve for h_1 and h_2,

$$h_2 = \frac{1}{2}h\left(\frac{\eta_1 - \eta_2}{\eta_1 + \eta_2}\right), \tag{1.1.20a}$$

$$h_1 = h + h_2. \tag{1.1.20b}$$

1.1.4 Interface stability

As stated earlier, the reaction interface is presumed to be situated in the middle of the extraction channel at all times. In practice this is of course not always the case. Certain criteria should be met to make sure that the interface will be in the middle. The known criteria will be taken into account and will be discussed in this section[1].

Viscosity-dependent phase flow rate ratio The higher viscous liquid in the microfluidic chip has the tendency to occupy a larger part of the extraction channel [12]. When this is not compensated for the interface will obviously not be in the middle of the extraction channel. To thus compensate this fact a certain ratio between the flow rates of the two phases based on the viscosity of the two phases must be met. This ratio has experimentally been found by A. Pohar et al [12] as

$$\frac{Q_1}{Q_2} = \left(\frac{\eta_1}{\eta_2}\right)^{-0.76}. \tag{1.1.21}$$

Herein are Q_1, Q_2 the flow rates for the two phases. This equation, and thus the value of the power, is valid for parallel flow conditions and is more suitable for small viscosity ratios.

Maximum extraction length The flow rate ratio found earlier will only compensate for a certain length of the channel for the viscous force. Eventually the interface will move towards the lower viscous phase. The expression for the maximum length of the extraction channel for which the interface will lie in the middle of the channel is found by S. Goyal et al [8] as,

$$L = \frac{2dw^2\gamma\sin(\theta - 90^o)}{\alpha Q_{aq}\eta_{aq}\left[1 - \left(\frac{\eta_{org}}{\eta_{aq}}\right)^{0.34}\right]}. \tag{1.1.22}$$

Herein is d the height of the channel, w the half-width of the channel, γ is the interfacial tension, Q_{aq} the flow rate of the aqueous phase, η_{aq} the viscosity of the aqueous phase and θ the contact angle shown in figure 1.1.2. The expression for α is found to be

$$\alpha = \frac{22}{7}\mathcal{C} - \frac{65}{3} = \frac{22}{7}\frac{2(w+d)}{wd} - \frac{65}{3} \tag{1.1.23}$$

for a rectangular cross section of the channel according to S. Goyal et al [8]. Herein is $\mathcal{C}$ the ratio between the wetted perimeter squared and the area of the aqueous phase.

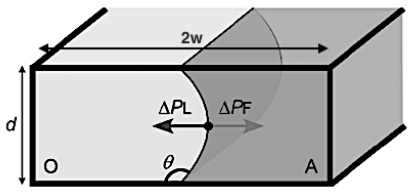

Figure 1.1.2: The interface between the organic phase (denoted with 'O') and the aqueous phase (denoted with 'A'). θ is the contact angle and d and w are the height and half-width used in equation 1.1.22. The arrows indicate the directions in which the pressures, pressure difference due to viscosity difference (ΔP_F) and Laplace pressure (ΔP_L), work.[2]

Reviewing the algebraic steps of the eventual formula reveals an algebraic error made by Goyal et al. Correcting this error results in the following algebraically right formula

$$L = \frac{2dw^2\gamma\sin(\theta - 90^o)}{\alpha Q_{aq}\eta_{aq}\left[1 - \left(\frac{\eta_{org}}{\eta_{aq}}\right)^{0.24}\right]}. \tag{1.1.24}$$

[1]Not all criteria are yet known. The known criteria are the ones mentioned in this report. Further research in this field can find new criteria, which should then be implemented in the model to make it more accurate.

Note that only the value of the power in the denominator changes from 0.34 to 0.24. On top of that in equation 1.1.23 it can be seen that S. Goyal et al included the interface-side of the aqueous phase to the wetted perimeter. This should be only the sides that make contact with the channel. Therefore, the expression for α should be

$$\alpha = \frac{22}{7}\mathcal{C} - \frac{65}{3} = \frac{22}{7}\frac{2w+d}{wd} - \frac{65}{3}, \tag{1.1.25}$$

instead of the expression shown in formula 1.1.23.

1.2 Mass Transfer

Knowledge about the mass transfer within the microchannel is needed to properly evaluate the movement of the metal ions and other species. First of all, general diffusion will be discussed with the help of Fick's law for diffusion and further on the mass transfer on an immiscible liquid-liquid interface will be discussed. At last the penetration theory will be introduced.

1.2.1 Fick's law for diffusion

Fick's first law considers the steady-state transport of mass due to diffusion. It relates the diffusive flux to the concentration with the assumption that this flux will flow from regions with high concentration to region with low concentrations. The magnitude of this flux is proportional to the concentration gradient and is scaled by the diffusion coefficient. This will lead eventually to the equation in one-dimension,

$$\frac{d^2\phi_m}{dt^2} = \phi_m'' = -\mathbb{D}\frac{dc}{dx}, \tag{1.2.1}$$

in which ϕ_m denotes the mass flow rate, $\mathbb{D}$ denotes the diffusion coefficient and c denotes the concentration. Equation 1.2.1 only holds when the system is binary and consists of a dilute solution. Furthermore, the molecules should not have high polarity or have non-spherical shapes [15].

Fick's second law considers the non-steady-state transport of mass due to diffusion. The second law predicts how the concentration will change with time. By taking the mass balance of a small area between x and dx with the use of equation 1.2.1 one will get [15],

$$\frac{\partial c}{\partial t} = \mathbb{D}\frac{\partial^2 c}{\partial x^2}. \tag{1.2.2}$$

1.2.2 Stokes-Einstein Equation for approaching diffusion coefficient

Einstein showed that the diffusion coefficient in an infinitely dilute solution can be describes as

$$\mathbb{D} = \frac{k_b T}{f}. \tag{1.2.3}$$

Herein is k_b Boltzmann's constant, T the temperature given in Kelvin and f the frictional coefficient of the diffusive particle. In general f is unknown, but George Stokes found an equation for the special case of a spherical particle of radius r which is moving in an uniform velocity in an continuous fluid of viscosity η. This lead to the equation

$$f = 6\pi\eta r. \tag{1.2.4}$$

If equation 1.2.4 also holds for spherical molecules than together with equation 1.2.4 one will get

$$\mathbb{D} = \frac{k_b T}{6\pi\eta r}. \tag{1.2.5}$$

With equation 1.2.5 an estimation of the diffusion coefficient can be made if the above described conditions are met.

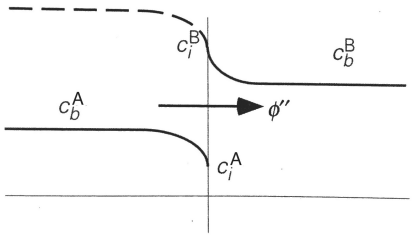

Figure 1.2.1: Two immiscible solutions with the same dissolved substance meet at the two-phase flow interface. At the interface an equilibrium, mentioned in equation 1.2.8 has been set. A diffusive flux will flow from left to right indicated with the arrow and the symbol ϕ''. [15]

1.2.3 The partition coefficient

To better understand the work of A. Blok [4] the important mechanism on which non-active liquid-liquid extraction is based must be discussed. Liquid-liquid extraction is based on the transfer of diluted species. When two immiscible solutions (respectively A and B) brought in contact eventually a concentration equilibrium of the dissolved substance will be present. In general, the concentrations in both solutions will not be the same, even though an equilibrium has set. This is due to the equality in the chemical potential of the dissolved substance in each solution [15]. Still no mass transfer may take place in an equilibrium state, so somehow the difference in concentration must be set to zero. This is done by introducing the partition coefficient m and is defined as,

$$m = \left[\frac{c^A}{c^B}\right]_{equilibrium}. \tag{1.2.6}$$

So with introducing this partition function the difference in concentration is zero,

$$0 = c^A - m \cdot c^B. \tag{1.2.7}$$

Herein c^A is the concentration of the dissolved substance in solution A and c^B is the concentration of the dissolved substance in solution B.

When there is no equilibrium (so a difference in chemical potential) a mass transfer will take place across the interface. On the interface, there will be an instantaneous equilibrium,

$$c_i^A = mc_i^B, \tag{1.2.8}$$

in which c_i^A is the concentration of the dissolved substance in solution A at the interface, and mc_i^B is the concentration of the dissolved substance in solution B at the interface. This can be seen in figure 1.2.1. Now at the bulk of both solutions there will be no equilibrium anymore. This will result in a mass transfer from the bulk of solution A to the interface and from the interface to the bulk of solution B. These two fluxes can be written down as,

$$\phi''_A = k_A(c_b^A - c_i^A), \tag{1.2.9a}$$
$$\phi''_B = k_B(c_i^B - c_b^B). \tag{1.2.9b}$$

Herein is k_A the mass transfer coefficient of the dissolved substance in solution A and k_B the mass transfer coefficient of the dissolved substance in solution B. These two fluxes should be equal due to the fact that the interface cannot collect any mass. With this knowledge and with the help of equation 1.2.8 the overall diffusive flux will be,

$$\phi'' = \left[\frac{1}{k_B} + \frac{m}{k_A}\right]^{-1}(mc_b^A - c_b^B) = \left[\frac{1}{mk_B} + \frac{1}{k_A}\right]^{-1}(c_b^A - \frac{1}{m}c_b^B) \tag{1.2.10}$$

One of the two terms within the brackets can be neglected if the ratio of the two reaches a certain value. This ratio is known as the Biot number and is described as,

$$Bi = \frac{\frac{1}{mk_B}}{\frac{1}{k_A}} = \frac{k_A}{mk_B}. \tag{1.2.11}$$

So, for knowing in which phase the resistance against the flux lies, one has to know k_A, k_B and m.

1.2.4 Penetration theory at an interface

When two immiscible phases are brought together a solute dissolved in one phase, let say phase A, will diffuse into the other phase, phase B, if possible. When the phase B does not contain a concentration of the solute at time $t = 0$ then the penetration theory is applicable. With the penetration theory, it is possible to make a rough analytical calculation how far the solute has penetrated phase B. This can be done by the equation

$$L_{pen} = \sqrt{\pi \mathbb{D} t}. \tag{1.2.12}$$

Herein is t the penetration time after $t = 0$. The theory is only applicable for small values of t for which the diffusion is constant and equal to the value on $t = 0$. When this is no longer the case and thus the diffusion has weaken due to the now present concentration of the solute in phase B the penetration theory is no longer applicable. This is when the penetration depth is 0.6 times the width of phase B. Note that if one still uses the penetration theory for depths bigger than this value an overestimation will be made. This is because the flux will always be the highest when no concentration is present in phase B.

1.3 Liquid-Liquid Extraction

Liquid-liquid extraction is a separation method that is built on the difference in solubility of chemical species, further referred to as solute, in certain liquids [1]. Active liquid-liquid extraction is basically the same as the non-active variant, only this method is not specifically build on the solubility. This method uses an extractant to selectively separate the solute. This research will focus on a potential ligand known as HOBO and hydroxyoximes as extractant. In this section, parallel flow non-active and active liquid-liquid extraction will be discussed.

1.3.1 Non-active parallel flow liquid-liquid extraction

As the name itself already partly suggests, this method uses two immiscible phases that are flowing parallel to each other. One phase contains the to be separated solute, normally this is the aqueous phase. The other phase, the organic phase, is used to extract the solute from the aqueous phase. This extraction is based on the diffusion of the solute. As discussed in section 1.2.3 the concentration of the specie in the aqueous and organic phase on the liquid-liquid interface differ by a coefficient known as the partition coefficient, indicated with m. Due to this phenomenon the solute concentration in the aqueous phase, in equilibrium, will be m times lower than the concentration in the organic phase. This is why, eventually more solute is present in the organic phase and is therefore effectively separated.

1.3.2 Active parallel flow liquid-liquid extraction

As stated earlier, the active variant used in this research is based on the selectivity of an added extractant to the organic phase. In this research, hydroxyoximes and the potential ligand HOBO will be discussed as extractants. HOBO is a specific hydroxyoxime on which there will later be elaborated on. Studies like [3] have shown that choosing the right circumstance for a specific hydroxyoxime can raise its selectivity for a particular metal. In the process of separating metals this is a real valuable characteristic.

As said, in this case the extractant resides in the organic phase. For most cases the extractant is insoluble in the aqueous phase, so the reaction with the metal will solely occur at the liquid-liquid interface. The general extraction of a metal, dissolved in a diluted acidic aqueous sulfate solution, with hydroxyoximes containing phenolic groups can, according to J. Szymanowski [14], be written as

$$M^{n+} + n\overline{HR} \Leftrightarrow \overline{MR_n} + nH^+. \tag{1.3.1}$$

M represents the metal, n stands for the molar ratio of ligand to metal complex. The overline indicates that the species are in the organic phase. The resulting product, MR_n, is in this case also not soluble in the aqueous phase. This technically means that all the reacted metal will thus remain in the organic phase, fully extracted from the aqueous phase.

The extraction constant for this extraction reaction can be found by

$$K_{ex} = \frac{\overline{[MR_n]}[H^+]^n}{[M^{n+}]\overline{[HR]}^n}. \tag{1.3.2}$$

In this case, the straight brackets indicate the concentration of the species in mol/m^3.

1.3.3 Selectivity of copper(II) with HOBO

2-Hydroxy-4-n-octyloxybenzophenone oxime (HOBO) is a good potential extraction ligand for copper(II) due to its high selectivity for only copper(II) over other base metals such as nickel(II) and cobalt(II)[8]. This high selectivity is caused by the introduction of an alkoxyl group to the phenyl group of hydroxyoximes which are typically used as extraction ligands for metal ions. Adding this group causes a lowering of the dissociation constant of phenol. As the word dissociation suggest this constant represents the extent to which the molecule is dissociated. A lower value means less dissociation.

1.3.4 Extraction reaction HOBO with copper(II)

The overall reaction which specifies the interaction with copper and HOBO is known as [3]

$$Cu^{2+} + 2\overline{HR} \Leftrightarrow \overline{CuR_2} + 2H^+; K_{ex}. \tag{1.3.3}$$

HR represents the HOBO. K_{ex} is the extraction equilibrium constant. The value for this dimensionless equilibrium constant was found to be 1.1×10^{-1} by the work of Baba [3]. In the work of S. Goyal et al [8] the copper ions diffuse slower than the reaction is taking place. The diffusion is thus the limiting factor for this situation. Exact knowledge of the reaction rate is therefore not necessary to obtain reliable results. To better understand this, consider the more striking example of a delivery man delivering packages. The delivery man can't deliver the packages quicker than they arrive, thus as long as he delivers the packages quicker than they arrive his actual speed is of no importance. This can also be verified by the Damköhler II number. This number gives the value for the ratio between the reaction rate and the diffusive mass transfer rate [10],

$$Da_{II} = \frac{k_r w^2}{\mathbb{D}}. \tag{1.3.4}$$

Herein is w the half-width of the extraction channel. Also, J. Szymanowski shows in table III.34 that mass transfer is the limiting step in this liquid-liquid extraction [14].

2 | Method

2.1 General Extraction Process Overview

2.1.1 The extraction process

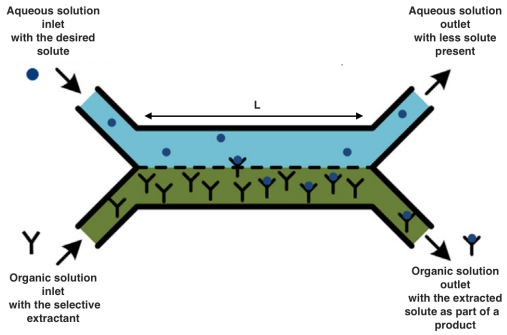

Figure 2.1.1: Image of the double Y-shaped microfluidic chip. An aqueous solution with metal ions is flowing in at the top. At the bottom an organic solution with an extractant is let in. Ideally at the end the organic solution only contains metal ions bound to the extractant. The length of the extraction channel is indicated with 'L'[8].

In order to obtain small amounts of copper a double Y-shaped microfluidic chip will be used which can be seen in figure 2.1.1. One inlet will contain an aqueous solution with a specific solute, whereas the other inlet contains an organic solution which can contain a specific extractant. The two phases are at any time immiscible. After flowing through the inlets, the two phases will flow into the extraction channel, the middle part of the microfluidic chip. In this extraction channel an interface will establish between the two immiscible liquids. In this research, it is assumed that this interface is perfectly centered in the middle. This will result in the fact that both phases are collected separately at the outlets, as can be seen in figure 2.1.1. Studies like [8], [9], [13], [12] show that several conditions, like a maximum extraction channel length and a viscosity-dependent flow rate ratio between the two phases, should be met in order to obtain in practice an interface perfectly centered in the middle. These conditions will be taken into account to make the assumption more valid.

To verify for which parameters the copper ions are separated the best a numerical model will be used. This will be done with the help of COMSOL®. The software is based on the finite element method. The finite element method in the 2D case divides the field of study into a series of controlled surfaces. These controlled surfaces are referred to as discretization. The partial differential equations which it must solve for can be approximated based on this discretization with numerical model equations. These last equations can be solved using numerical methods and will be solved for every part of the discretization [7]. The discretization pattern can be adjusted to the geometry. The denser it gets, the more computation time it requires. In this research, it is chosen to make the discretization, further referred to as the mesh, denser in the middle of the channel. This is done the reaction happens at the interface and should therefore be calculated more detailedly. The mesh can be seen in figure 2.1.2.

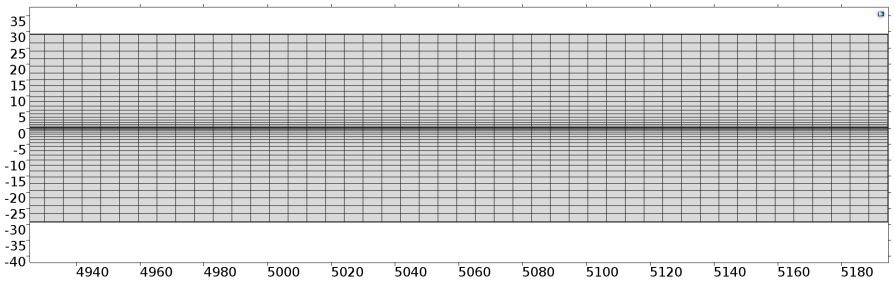

Figure 2.1.2: Meshing of the geometry used in this research. The mesh is more dense towards the interface in order to detailedly calculate the reaction happening at the interface. The interface is located at y=0.

2.1.2 Process simplifications

The process described above is evaluated in 2D to reduce computation time. Nevertheless, it will presumably not greatly influence the results. This can be assigned to the fact that the interest is in the percentage of copper extracted and not in the absolute amount of copper. This assumption will be evaluated by comparing some 3D results to the 2D results.

As mentioned earlier, the microfluidic chip contains a Y-shape for both the inlets and outlets. For this research, it is not necessary to take these into account when making the model, because the separation processes that is investigated takes exclusively place in the extraction channel. Thereby the flow will be assumed to be fully developed throughout the entire extraction channel. This is plausible because the distance that is needed in order for the two phases to gain a fully developed state can be considered negligibly small. The computation time will as well benefit from the fact that the in- and outlets are kept out of consideration.

More on the flow profile is the way in which it is modelled. With some effort, a plug flow profile can be created in a microfluidic chip. This model however will consider a laminar flow profile due to a statement made by B. Malengier et al [11] that a plug flow profile will result in a poorer performance compared to a laminar profile.

To ensure that the interface stays in the middle of the geometry a fake two-phase flow will be modelled. This is done by modelling a one-phase flow and define the viscosity and the density space-dependent. So let's say that the interface will be on $y = 0$ then the viscosity and density will differ for the area $y > 0$ and $y < 0$. To make this clearer an illustration can be found in figure 2.1.3.

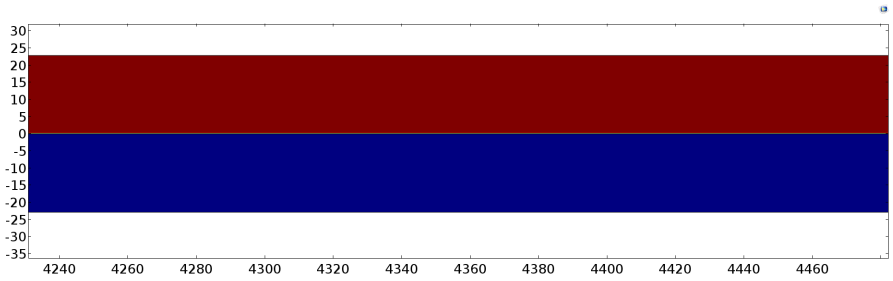

Figure 2.1.3: The viscosity and density dependent geometry. The red colour illustrates the aqueous phase and the blue colour illustrates the organic phase. The interface is located at y=0.

2.1.3 Modelling of the non-active liquid-liquid extraction

The non-active liquid-liquid extraction cannot directly be modelled with COMSOL. This is because COMSOL does not take the solubility of the solute in both phase into account, due to the fact that the two-phase flow is modelled as a modified one-phase flow (see section 2.1.2). The workaround for this is done by allocating to each phase a separate "Transport of diluted species" module. For both modules, a flux boundary condition will be added to the interface boundary. For the aqueous phase, phase A, the flux expression will be

$$N_{0,[A]} = k\left(\frac{[A]}{m} - [B]\right). \tag{2.1.1}$$

Herein is $[A]$, $[B]$ the concentration of the solute in respectively phase A and B, m represents the partition coefficient and k denotes the mass transfer coefficient. The flux expression for the flux boundary condition for the organic phase, phase B, will then be

$$N_{0,[B]} = k\left([B] - \frac{[A]}{m}\right). \tag{2.1.2}$$

This boundary condition definition will now account for the needed concentration difference, which manifest immediately at the surface and eventually throughout the whole system when in equilibrium. Note that this should as well be implemented in the active liquid-liquid extraction model when the solute is individually (read: not exclusively as a part of a product formed by a reaction) present in the organic phase.

2.1.4 Modelling of the active liquid-liquid extraction

As discussed earlier, the active liquid-liquid extraction will be modelled for the ideal case. This means that the reaction is irreversible, the extractant is present is such high concentrations that it can be considered constant, the product which arises from the concentration will not diffuse into the aqueous phase and the reaction rate is high such that the whole process is diffusion limited. Note that modelling the process in this way means that eventually 100 percent extraction could be achieved, which could in practice turn out to be harder to achieve. It is accomplished by using COMSOL's "Chemistry" module to define the reaction and the species involved. Next the concentration of each specie at the inlet is defined in the "Transport of diluted species" module and this module then accounts for all the species when calculating the mass transfer. Furthermore, a boundary condition called "Thin diffusion barrier" is defined on the interface. This boundary defines which species can pass the interface. In this case only the solute can pass the interface in order to obtain the ideal situation.

3 | Results and Discussion

This section is divided into several parts. First of all, the assumption that the active liquid-liquid extraction variant is more effective than the non-active variant is elaborated and shown on the hand of a study done by A. Blok [4]. Next to this it will also be shown that a laminar flow profile inside the extraction channel compared to a plug flow profile will result in better performance, which was investigated by B. Malengier et al [11].

From there the simplification of the model by modeling in 2D is justified by comparing the extraction rate of a 3D model to the 2D model. After this justification, the model on its own should be proven of its correctness. This is done by comparing it with a study of interest namely a study done by S. Goyal et al [8]. This study uses a potential ligand which is highly selective for copper. This selectivity is especially valuable for extraction processes in which a high amount of metal pollution is present in the aqueous phase.

With the capabilities of the model known a parametric sweep is made for the tunable parameters of the microfluidic chip and the phases involved. From this data, the overall and the qualitative influence of the parameters will be shown.

3.1 Assumption Evaluation

3.1.1 Active liquid-liquid extraction more effective

As mentioned earlier, the non-active liquid-liquid extraction depends on the higher solubility of the solute in the aqueous phase. Due to this solubility difference a higher concentration of the solute will eventually be present in the organic phase. Something which can be seen in figure 1.2.1. Something which can also been seen from this figure is the fact that there will always be a bit of concentration present on the interface of the aqueous phase. The lower the concentration at the interface the bigger the gradient will be and hence the flux to interface will be higher.

The active variant is based on a interfacial reaction between the solute and the extractant. Assume the ideal situation in which the reaction is irreversible, the extractant is present in such high concentrations that it can be assumed constant and the reaction rate is much higher than the diffusion. In this case, all the solute arriving at the interface will immediately react and establish a zero concentration at the interface. A situation which cannot be achieved with the non-active variant. The situation where the concentration of the solute is zero at the interface creates the highest possible concentration gradient and thus the highest flux towards the interface. This will obviously be a favourable situation and therefore the active variant is assumed to be more effective.

A study done by A. Blok [4] investigates the separation of Technetium-99m with a parallel flow non-active liquid-liquid extraction in a microfluidic chip. The flow through the chip was modelled by a plug flow model. The research treats several different cases for the extraction process. Three of these cases have been used to test the assumption. The properties which are at all time to each system applicable can be found in the first few rows of table A.1 in the results appendix. At the end the parameters for the three cases are listed. One of these parameters is the extraction length, which is maximum extraction channel length calculated with formula 1.1.24.

In table 3.1 the extraction rate found by A. Blok is compared with the extraction rate found by the non-active model created in this research. The extraction rate is calculated following

$$ER(\%) = \left(1 - \frac{C_{out}^{aq} \cdot Q_{out}^{aq}}{C_{in}^{aq} \cdot Q_{in}^{aq}}\right) \cdot 100, \tag{3.1.1}$$

in which C_{out}^{aq} indicates the remaining concentration of the solute in the aqueous phase at the aqueous outlet and C_{in}^{aq} indicates the begin concentration of the solute in the aqueous phase at the

aqueous inlet. Q_{out}^{aq} symbolizes the aqueous flow rate at the aqueous outlet and Q_{out}^{aq} represents the aqueous flow rate at the aqueous outlet. From this table, it can be seen that the models show somewhat the same results, which indicates that the created model simulates the situation in a correct way.

Table 3.1: Results for the three different cases selected from the study done by A. Blok [4]. It concerns a non-active liquid-liquid extraction with a plug flow profile.

Non-active liquid-liquid extraction with a plug flow		
Case	Extraction Rate	
	A. Blok (%)	Current (%)
1	64	63
2	44	43
3	27	26

In table 3.2 the extraction rates for the three cases when the active liquid-liquid extraction process with the same properties is modelled can be seen. The extraction rates do not differ, which does not agree with the assumption. The partition coefficient used in the study by A. Blok is high, namely 778. This will lead to a concentration of the solute at the aqueous side of the interface approaching zero. This can be seen from figure 3.1.1. Figure A.1 shows the concentration profile over the full width of the channel and it looks like the concentration is zero at the interface, but when zooming in as done in figure A.2 the concentration does not reach zero. From this same figure for B.2 it can be seen that for the active variant the concentration reaches zero at the interface. This does agree with the assumption. This concludes that a non-active variant with a very high partition coefficient will come close to the ideal active variant, but the ideal active variant will always be slightly better.

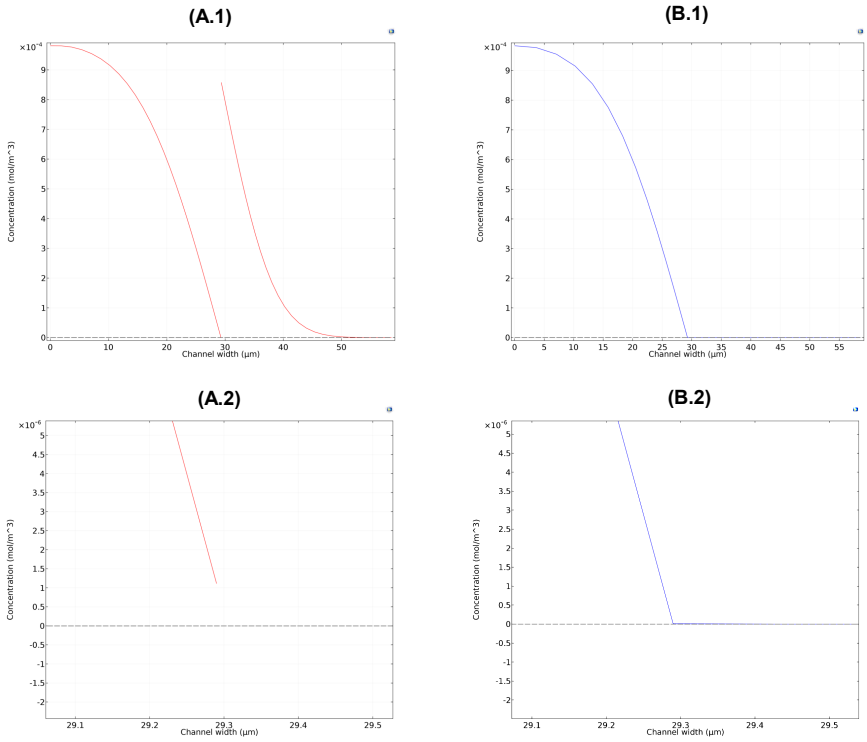

Figure 3.1.1: The concentration profiles in the middle of the channel for case 2 for (A) the non-active variant and for (B) the active variant. Figure A.1 and B.1 show the concentration profile on the whole width of the channel and figure A.2 and B.2 show the concentration profile zoomed in at the interface.

Table 3.2: Results for the three different cases selected from the study done by A. Blok [4]. It concerns an active liquid-liquid extraction with a plug flow profile.

Active liquid-liquid extraction with a plug flow	
Case	Extraction Rate
1	63
2	43
3	26

3.1.2 Laminar flow profile for better performance

Furthermore, the previous results were obtained for a model with a plug flow velocity profile. Because a study by B. Malengier et al [11] found that a microfluidic chip gives poorer performance when a plug flow profile is present it is valuable to verify this statement. In table 3.3 the results for the same cases modeled with a laminar flow profile is depicted. From these results, it can indeed be seen that the extraction rate raises when a laminar flow profile is present in the extraction channel. The model thus agrees with the statement made by B. Malengier et al. A laminar profile will therefore be used in the later model for the parametric sweep.

Table 3.3: Results for the three different cases selected from the study done by A. Blok [4]. It concerns an active liquid-liquid extraction with a laminar flow profile.

Active liquid-liquid extraction with a laminar flow	
Case	Extraction Rate
1	66
2	46
3	28

3.1.3 2D modeling to reduce computation time

Downgrading the models from 3D to 2D will save a substantial amount of computation time. In order to apply this downgrade, it must be verified that the results do not differ in both cases. The second case of table 3.3 is remodeled in 3D to compare the results of the different dimensions. In table 3.4 the results can be seen. As expected the results do not substantially differ, so using a 2D model is a safe way in order to reduce computation time. This result is valuable because computing the 2D model took 4 minutes, where the 3D model took 44 minutes.

Table 3.4: Comparison of the extraction rate of the 2D model and the 3D model

Extraction rate	
2D (%)	3D (%)
46	47

3.2 Model Evaluation

3.2.1 Active liquid-liquid extraction with the potential ligand HOBO

To verify if the active liquid-liquid extraction model, which is also used to obtain the results in section 3.1.1, works correct the work of S. Goyal et al [8] is helpful. This study separates copper with an active liquid-liquid process. The extractant which is used is known as 2-hydroxy-4-n-octyloxybenzophenone oxime, abbreviated as HOBO and its reaction is fast so the whole process is diffusion limited. The study measured the extraction rate in practice and verified their result by a model made in COMSOL.

In table A.2 in the results appendix the parameters for the circumstances in which the active liquid-liquid extraction was performed, mentioned by S. Goyal et al in their supplementary information appendix, can be found. The results for the extraction process for both the study by S. Goyal et al and the model made in this research are displayed in table 3.5.

Table 3.5: Results for the extraction rate and the extraction time for the extraction process done by S. Goyal et al [8] and for the model made in this research.

Extraction rate (%)	
S. Goyal	Current model
>95	10
Extraction time (s)	
S. Goyal	Current model
0.21	0.21

The extraction time mentioned in table 3.5 is calculated by

$$t_{ex} = \frac{Ldh}{Q_{aq}}. \tag{3.2.1}$$

It is the average residing time of the solute in the extraction channel.

Where the study by S. Goyal et al claims an extraction rate often exceeding 95% this study found that it would not exceed the 10%. This certainly raises questions about the reliability of the model. In order to make an estimation if the model did exactly fail to simulate this a rough analytical approach must be done.

Because the process is diffusion limited the amount of solute, in this case copper, that can diffuse to the interface within the time that it resides in the extraction channel will be a good measure. To reach an extraction rate which exceeds 95% also the upper copper species must have been diffused to the interface. Because convection only happens in the positive x-direction (parallel to the length of the extraction channel towards the outlets) the movement of the copper species towards the interface solely depends on diffusion. As S. Goyal et al states the residing time was 0.21 seconds. With the penetration theory, discussed in section 1.2.4, an estimation can be made how far these upper copper species could have diffused towards the interface. The penetration theory is obviously not applicable anymore, but as it is known that this method will lead to an overestimation it can give an upper boundary for the penetration depth. Using formula 1.2.12 and filling in the value 0.21 seconds for the variable t and for $\mathbb{D}$ the value stated by S. Goyal et al, which can also be found in table A.2 of the results appendix, the penetration depth will be 30 μm. Considering the fact that the aqueous phase is 200 μm wide (half the full-width of the extraction channel) the uppermost copper species can never reach the interface. On ground of this rough estimation the conclusion can be made that in the way this research interprets the results stated by S. Goyal et al the 95% extraction rate can never be achieved. The 10% however seems way more plausible. Probably some crucial information is overlooked or the information is not given by S. Goyal et al. There is thus no reason to assume that the created model is incorrect.

Furthermore, as stated in section 1.1.4, S. Goyal et al made an algebraic error in their formula for the maximum extraction channel length. On top of that also the wetted perimeter was calculated incorrectly. These two mistakes point out some carelessness during the research process, which could explain the substantial difference in the results.

3.3 Parametric sweep for optimized microfluidic chip

Because extraction processes are only of value when a substantial part of the desired solute has been extracted it is important to know which setup for an active liquid-liquid extraction will result in a high extraction rate. Due to the evaluation of the correctness of the model it is now possible to gain insights in the influence of different kind of parameters on this extraction rate. The parameters of interest will be

1. viscosity of aqueous phase (η_{aq}),
2. viscosity of the organic phase (η_{org}),
3. aqueous flow rate (Q_{aq}) (taking into account equation 1.1.21),
4. extraction channel length (L),
5. extraction channel full-width (h),
6. extraction channel height (d),
7. diffusion coefficient of solute in the aqueous phase ($\mathbb{D}_{aq}$).

Point 4 mentioned in the list is limited to a maximum of one centimeter in order to keep the channel maintainable on a microfluidic chip. Note that it is not possible to easily change the value of the diffusion coefficient, point 7, of a solute in the aqueous phase. The purpose of adding this parameter is to gain insights in the impact of this value on the extraction rate and to make the results for a wider range of situations applicable. Table 3.6 shows the different values of the parameters over which the system is swept. All values will be combined with one and other to obtain a total overview of the parameter relations.

Table 3.6: Values for the parameters mentioned in the enumeration in this section. All parameter values will be combined with each other in order to obtain a full overview.

Parameter	Unit	Values		
Phase parameters				
η_{aq}	$mPa \cdot s$	0.6	0.8	1
η_{org}	$mPa \cdot s$	0.3	0.4	0.5
Q_{aq}	m^3/s	$2.5 \cdot 10^{-10}$	$3 \cdot 10^{-10}$	$3.5 \cdot 10^{-10}$
$\mathbb{D}_{aq}$	m^2/s	$1 \cdot 10^{-8}$	$1.5 \cdot 10^{-9}$	$1 \cdot 10^{-9}$
Dimension parameters				
h	μm	40	70	100
d	μm	40	70	100
L	mm	5	8	10

In table A.3 a part of the results are shown for when the aqueous viscosity stays constant with a value of 1 $mPa \cdot s$ and the diffusion coefficient varies from 0.1 to 0.15 m^2/s . The results are filtered on the highest extraction rate and cut-off when every parameter has changed value one time. From this the absolute and relative influence on the extraction rate of each parameter can be deduced. In table A.3 the first change in each parameter value is indicated and in table 3.7 the absolute and relative changes to the parameter value and the associated absolute and relative values for the extraction rate are indicated.

Table 3.7: Relative and absolute change in the parameter value and in the resulting extraction rate when parameter changes value for the first time shown in table A.3.

P		Δ_{abs}	Δ_{rel} (%)	ER_{abs}	ER_{rel} (%)
η_{org}	$(mPa \cdot s)$	0.40	66.67	3.21	4.69
Q_{aq}	(m^3/s)	0.50	16.67	5.31	8.00
L	(mm)	0.20	25.00	6.50	9.98
d	(μm)	30	30.00	10.27	16.74
h	(μm)	30	42.86	15.89	22.70
$\mathbb{D}_{aq}$	(m^2/s)	0.050	50.00	11.63	19.40

4 | Conclusions

This section will make conclusion based on the data obtained by the parametric sweep. Firstly, the general influence of the parameters will be explained and eventually the qualitative conclusions on the influence of each parameter will be made.

4.1 General conclusions on parametric sweep

The average extraction data for each parameter value is useful to make some general conclusions. Starting of with the dimensions of the extraction channel followed by the more phase specific parameters.

4.1.1 Influence of dimensions

As can be seen from figure A.3.1 in the result appendix the extraction rate grows when the extraction length is increased. This can be logically declared because extending the length of the channel increases the average residing time of the solute. This means that eventually more solute can diffuse to the interface and can react with the extractant. Keep in mind that the maximum length of the extraction channel is calculated with equation 1.1.24. A too large channel length can thus dislocate the interface from the middle of the channel.

Decreasing the width of the channel causes raise in the extraction rate. This can be declared in the same way, but it is a bit more complicated. A decrease in the width means a decrease of the average distance to the interface, but increases the velocity inside the extraction channel. The smaller distance to the interface is favourable for the amount of solute eventually diffusing to the interface, but the higher velocity is unfavourable. Clearly the distance decrease has far more impact than the increase in velocity and thus the extraction rate raises.

The height of the channel deals with the same changes as changing the width of the channel. Increasing the height of the channel will increase the size of the interface, so the reaction surface increases. Furthermore, increasing the cross-sectional area of the channel will decrease the velocity. A decrease in velocity means that the solute's diffusive penetration depth to the interface is enlarged. So, increasing the cross-sectional area while keeping the average distance to the interface (read: width) low will have a positive effect on the extraction rate.

4.1.2 Influence of phase parameters

The velocity inside the channel can also be reduced by lowering the flow rate value, which leads to, as discussed previously, an increase in extraction time. It is good to notice that a too low flow rate can cause the interface to be dislocated from the middle of the channel. This is not the case according to the formula for the maximum extraction channel length, but it is found in the study by A. Blok [4]. Droplets are created in the channel and there can no longer be talked of a two-phase flow. In an ideal situation, a low flow rate will increase the maximum channel length and will expand the average residing time. Keeping the flow rate as low as possible is thus contributory to a high extraction rate.

Raising the diffusion coefficient will enlarge the solute's diffusion path length and thus raise the eventual extraction rate. Finding an aqueous solution or some method for which the diffusion coefficient of the solute is significantly higher is thus a great benefit for the eventual extraction rate.

The model shows that raising the value for the organic viscosity relative to the aqueous viscosity will increase the extraction rate. This can be declared by formula 1.1.21 which is taken

into account by calculating the organic phase flow rate in order to establish a stable interface. When the organic viscosity raises and the aqueous viscosity stays the same then the organic flow rate will decrease. A decrease in the organic flow rate will lower the velocity within the channel and therefore also the velocity at the interface. A lower velocity at the interface will therefore cause a longer contact time and thus a higher extraction rate.

4.2 Qualitative conclusions on parametric sweep

Analysing the data a bit more thoroughly reveals the impact of every parameter when changed. In table A.3 the data for a part of the parametric sweep is shown. From this table, the relative impact of the parameters can be established. The last row of the table shows the most efficient setup, which could have been predicted from the analysis done in the previous section. Every time a parameter changes for the first time it can be seen that all other parameters obtain their optimal value. From this it can be concluded that changing viscosity of the aqueous phase is the least efficient. Changing it from 0.6 to 1 $mPa \cdot s$ only raises the extraction rate in this case with about 3 percent. In table 3.7 this has been worked out for every parameter together with the relative changes. From this and knowledge about the limitations of every parameter it can be deduced for which parameters it is the most valuable to overcome the known limitations.

The length, height, width and the diffusion coefficient show the highest amount of influence on the extraction rate. The diffusion coefficient and the height of the channel are left out of consideration because the diffusion coefficient can generally not be changed and raising the height beyond the currently used maximum value will stimulate the droplet formation substantially. For the length on the other hand research is now being done to look for a hydrophobic coating which could be used inside the channel for the organic phase to make extending the length of the extraction channel possible. This research is still facing a lot of complications, but it is a start. Narrowing down the width shows the highest amount of relative change in extraction rate, therefore it will be the most valuable to overcome the limitation on the parameter. This is hence the reason why the focus is as well on the width of the channel.

Table A.4 in the results appendix shows what would happen if the value for the length and the width go beyond their limitation. When an extraction channel with a length of 4 cm is used an extraction rate of approximately 99 percent can be reached when keeping the other parameters at their optimal values. When the width is lowered to 20 μm the extraction rate will raise to a value of 90 percent. These results confirm the assertion that overcoming the limitations on these parameters will open a bright future for active liquid-liquid extraction in a microfluidic chip.

5 | Recommendations

The results found in this research are proven to be significant, but there were some restrictions and assumptions made in order to fit the available research setup to the research possibilities. Therefore, in reality the results will not always match or will not be applicable to all situations. This section will discuss the shortcomings of this research and will elaborate on the possibilities for further research

First of all, the assumption that the interface is located exactly in the middle of the channel will not always be true. For example, for low flow rates observed by A. Blok [4], too long extraction channels discovered by S. Goyal et al [8] and for high viscosity ratios the equation 1.1.21 found by A. Pohar et al [12] is no longer applicable. Implementing more restrictions like these to the model too ensure the interface is located in the middle will enforce the final results. Nonetheless some of these restrictions are still being investigated and thus the question on why the interface gets dislocated from the center is not fully answered yet. As soon as this is known it will be valuable to add these to the model. Moreover, the model can with better knowledge of these restrictions be modelled as an actual two phase flow. Keep in mind that this model uses a 'fake' two phase flow, which models a one phase flow with dimensional conditions for the density and the viscosity of the phase.

Another assumption which is made, is the fact that the solute will not be found individually present in the organic phase, but only as a product of the reaction happening at the interface. For most of the liquid-liquid extraction setups this will be applicable, but for some case where the reaction rate is the limiting factor and the solute may dissolve in the organic phase it is not. To also predict these special cases with a high accuracy the model must take the partition coefficient into account. Implementing this with the help of COMSOL can be a difficult task, but maybe future releases will provide for a solution.

Next up is the restriction in dimensions. Modelling the geometry in 2D was proven to be a good computation time reducing solution to find the extraction rate of the different setups, but gives less insight in the actual behaviour of the phases inside the channel. The interface that establish is not flat as is assumed in this research. Due to the interfacial tension the interface will be curved, which can be seen in figure 1.1.2. A curved surface will cause an increase in the contact area and thus an increase in extraction rate. A 3D model was already created in this research, but was only used for verification of the earlier mentioned assumption because of the excessive computation time. Upscaling the model from 2D to 3D is thus an important extension to take the phase behaviour into account.

The active model has not been tested for more studies than the study of S. Goyal et al. Next to the analytical approximation to determine the reliability of the model testing it to another known study would increase its credibility even more. Finding a similar study to test the model with would therefore a valuable additional check.

The focus in this research is on the separation of metal ions. That is why the process for hydroxyoximes is described. This reaction is specific for metals and therefore good applicable in this research. When other metals, like zinc, are present in the aqueous phase next to the desired solute it can cause difficulties in selectively separate the desired solute. A research which focuses on these hydroxyoximes and finding ligands that selectively separate specific metals like HOBO can be useful in this field of research. It seems that the structure of a hydroxyoxime plays a key role in this selectivity process, as stated by E. Oehlke[1]. This is what makes the potential ligand HOBO selective to copper. The copper ion has a characteristic that it likes to be present in a flat structure. Because knowledge about this field should come from chemical engineers it lays outside

[1]This statement has been made in an one to one consultation. The statement is therefore an interpretation of the researcher and should be checked with literature to verify plausibility.

the scope of this research, but investing additional time to this dependency within a new research would nonetheless be likely to bring some interesting and usable results.

Bibliography

[1] M. Aguilar and J. L. Cortina. *Solvent extraction and liquid membranes: Fundamentals and applications in new materials*. CRC Press, 2008.

[2] A. Aota, K. Mawatari, and T. Kitamori. Parallel multiphase microflows: fundamental physics, stabilization methods and applications. *Lab on a Chip*, 9(17):2470–2476, 2009.

[3] Y. Baba, M. Iwakuma, and H. Nagami. Extraction mechanism for copper(ii) with 2-hydroxy-4-n-octyloxybenzophenone oxime. *Industrial & Engineering Chemistry Research*, 41(23):5835–5841, 2002.

[4] A. Blok. Extraction of technetium-99m. 2015.

[5] H. Bruus. *Theoretical microfluidics*. Oxford University Press, 2007.

[6] D. Ciceri, J. M. Perera, and G. W. Stevens. The use of microfluidic devices in solvent extraction. *Journal of Chemical Technology and Biotechnology*, 89(6):771–786, 2014.

[7] COMSOL. Finite element analysis (fea) software. https://www.comsol.com/multiphysics/fea-software, 2017. Accessed on: 2017-08-15.

[8] S. Goyal, A. V. Desai, R. W. Lewis, D. R. Ranganathan, H. Li, D. Zeng, D. E. Reichert, and P. J. Kenis. Thiolene and sifel-based microfluidic platforms for liquid–liquid extraction. *Sensors and Actuators B: Chemical*, 190:634 – 644, 2014.

[9] G. Hellé, S. Roberston, S. Cavadias, C. Mariet, and G. Cote. Toward numerical prototyping of labs-on-chip: modeling for liquid–liquid microfluidic devices for radionuclide extraction. *Microfluidics and Nanofluidics*, 19(5):1245–1257, 2015.

[10] L. Janssen and M. Warmoeskerken. *Transport Phenomena Data Companion*. Edward Arnold, 2006.

[11] B. Malengier, J. Tamalapakula, and S. Pushpavanam. Comparison of laminar and plug flow-fields on extraction performance in micro-channels. *Chemical Engineering Science*, 83:2 – 11, 2012. Mathematics in Chemical Kinetics and Engineering International Workshop 2011.

[12] A. Pohar, M. Lakner, and I. Plazl. Parallel flow of immiscible liquids in a microreactor: modeling and experimental study. *Microfluidics and Nanofluidics*, 12(1):307–316, Jan 2012.

[13] P. J. Stiles and D. F. Fletcher. Hydrodynamic control of the interface between two liquids flowing through a horizontal or vertical microchannel. *Lab on a Chip*, 4(2):121–124, 2004.

[14] J. Szymanowski. *Hydroxyoximes and Copper Hydrometallurgy*. Taylor & Francis, 1993.

[15] H. van den Akker and R. Mudde. *Transport Phenomena*. Delft Academic Press, 2014.

[16] B. Wolterbeek, J. L. Kloosterman, D. Lathouwers, M. Rohde, A. Winkelman, L. Frima, and F. Wols. What is wise in the production of 99mo? a comparison of eight possible production routes. *Journal of Radioanalytical and Nuclear Chemistry*, 302(2):773–779, Nov 2014.

Appendices

A | Results Appendix

A.1 Assumption evaluation

Table A.1: Properties for the extraction process done in the study by A. Blok [4]. On the last 4 rows the different parameters for the 3 cases are mentioned. The cases will be referred by their corresponding number

Parameter	Value			Unit
Water				
η_{aq}	$0.890 \cdot 10^{-3}$			$Pa \cdot s$
$D_{99TcO_4^-}$	$1.48 \cdot 10^{-9}$			m^2/s
$[99TcO_4^-]$	0			mol/m^3
2-butanone (MEK)				
η_{org}	$0.405 \cdot 10^{-3}$			$Pa \cdot s$
$D_{99TcO_4^-}$	$1.09 \cdot 10^{-9}$			m^2/s
$[99TcO_4^-]$	10^{-6}			mol/m^3
Overall parameters				
γ	$48.2 \cdot 10^{-3}$			N/m
m	778			-
θ	108			degrees
Cases	1	2	3	
h	45.72	58.58	71.42	μm
d	100	100	50	μm
L	8.09	9.41	8.68	mm
Q_{aq}	$1.67 \cdot 10^{-10}$	$3.33 \cdot 10^{-10}$	$3.33 \cdot 10^{-10}$	m^3/s

A.2 Model evaluation

Table A.2: Properties for the extraction process done in the study by S. Goyal [8]. Footnotes indicate that the values are found outside the supplementary information appendix made by S. Goyal et al.

Parameter	Value	Unit
Aqueous Phase		
η_{aq}	$1.28 \cdot 10^{-3}$	$Pa \cdot s$
D_{Cu}	$1.32 \cdot 10^{-9}$	m^2/s
$[Cu]$[1]	$1 \cdot 10^{-11}$	M
$[HOBO]$	-	-
Q_{aq}	$3.33 \cdot 10^{-10}$	m^3/s
Organic Phase (Toluene)		
η_{org}	$0.59 \cdot 10^{-3}$	$Pa \cdot s$
D_{CuHOBO}[2]	$1 \cdot 10^{-9}$	m^2/s
$[Cu]$	-	-
$[HOBO]$	$1 \cdot 10^{-5}$	M
Q_{org}	$5.83 \cdot 10^{-10}$	m^3/s
Extraction Channel dimensions		
d[3]	400	μm
d	50	μm
L	7	mm
Overall parameters		
γ	$37.1 \cdot 10^{-3}$	N/m
θ	132	$^\circ$

[1] Found in the actual report on page 642 ("...the concentration of HOBO is almost six orders of magnitude larger than copper,...").
[2] Estimated.
[3] S. Goyal et al mentoins "...channels that 200 μm wide..." on page 641. Full-width is thus 400 μm wide.

A.3 Parametric Sweep

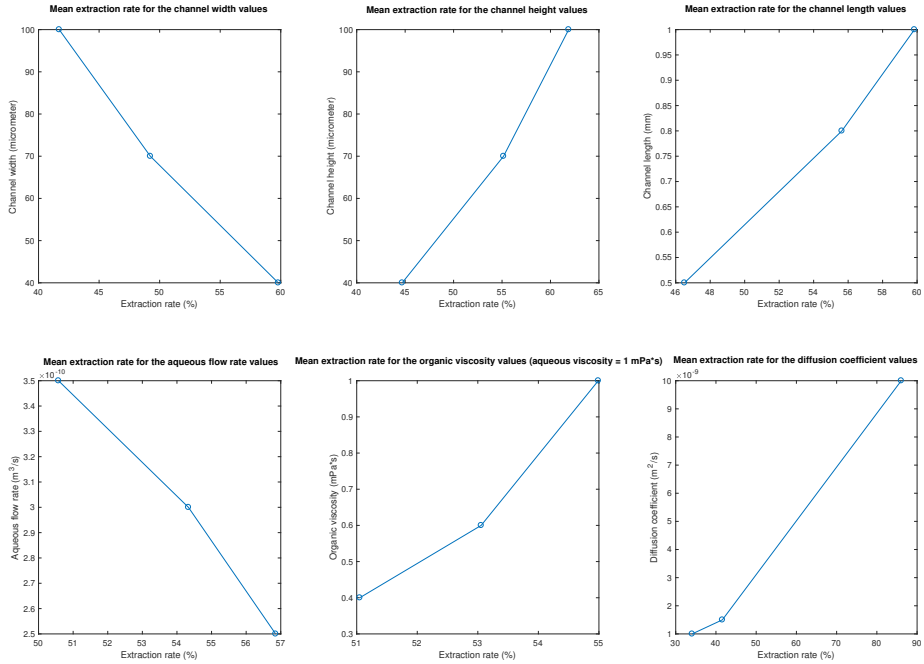

Figure A.3.1: Plot for the mean extraction average for the parameters.

Table A.3: Part of the results from the parametric sweep for the aqueous viscosity set to 1 $mPa \cdot s$ and the diffusion coefficient varying from 0.10 to 0.15 m^2/s shown. The results have been cut-off when every parameter has changed value one time. The yellow color indicates the value change.

h (μm)	d (μm)	Q_{aq} (m^3)	η_{aq} ($mPa \cdot s$)	η_{org} ($mPa \cdot s$)	L (mm)	$\mathbb{D}_{aq}$ (m^2/s)	ER (%)
70	100	2.5	1	1	1	0.15	55.73
40	100	3.5	1	1	0.8	0.15	55.82
40	100	3.5	1	0.4	1	0.15	56.01
40	70	3	1	1	1	0.15	56.38
40	100	3	1	0.6	0.8	0.15	57.11
40	100	2.5	1	0.6	1	0.10	57.17
40	70	2.5	1	0.6	1	0.15	58.38
40	100	3.5	1	0.6	1	0.15	58.92
40	100	2.5	1	0.4	0.8	0.15	59.10
40	100	3	1	1	0.8	0.15	59.98
40	100	2.5	1	1	1	**0.10**	59.99
40	100	3	1	0.4	1	0.15	60.14
40	**70**	2.5	1	1	1	0.15	61.35
40	100	3.5	1	1	1	0.15	61.92
40	100	2.5	1	0.6	0.8	0.15	62.09
40	100	3	1	0.6	1	0.15	63.19
40	100	2.5	1	1	**0.8**	0.15	65.12
40	100	2.5	1	0.4	1	0.15	65.24
40	100	**3**	1	1	1	0.15	66.32
40	100	2.5	1	**0.6**	1	0.15	68.41
40	100	2.5	1	1	1	0.15	71.62

Table A.4: Extraction rates shown for varying the length and the width independently. The other parameters are kept the same as the value shown in the last row of table A.3.

Value	ER (%)
L (cm)	
2	89.91
3	96.39
4	98.71
d (μm)	
20	90.43